Organic Process Research & Development **2004**, *8,* 725–737

Articles

A Pressure-Resistant Small-Scale Reaction Calorimeter That Combines the Principles of Power Compensation and Heat Balance (CRC.v4)

Fabio Visentin, Stefano I. Gianoli, Andreas Zogg, Oemer M. Kut, and Konrad Hungerbühler*

Safety and Environmental Technology Group, Laboratory of Technical Chemistry, Institute for Chemical and Bioengineering, Swiss Federal Institute of Technology (ETH), ETH Hoenggerberg, HCI G133, CH-8093 Zurich, Switzerland

Abstract:

An improved version of a small-scale reaction calorimeter fitted with an integrated infrared-attenuated total reflection (IR-ATR) probe has been developed. The new device has a sample volume of 20−50 mL, a metal block as an intermediate thermostat and is applicable to higher pressure up to 30 bar. Isothermal conditions are maintained using the power compensation principle. Peltier elements are implemented to compensate the change of the heat-transfer coefficient during the measurement, making time-consuming calibrations unnecessary.The Hastelloy reactor vessel is easily exchangeable and is available with and without the IR-ATR probe. The new combined reaction calorimeter (CRC.v4) has been characterized by using test reactions such as neutralization of NaOH, hydrolysis of acetic anhydride, and acetylation of a substituted benzopyranol. The characteristics of the new equipment and those of an earlier published version are compared.

Introduction

Reaction calorimetry is used to identify thermodynamic and kinetic parameters, which are crucial for design and optimization of chemical processes.

Most of the existing reaction calorimeters consist of a reaction vessel and a surrounding jacket with a circulating fluid that transports the heat away from the reactor. Such devices can be classified into three categories according to the measurement and control principles: heat flow, heat balance, and power compensation calorimeters.[1−3] Conventional reaction calorimeters are based on the heat flow principle, and more advanced devices use the heat balance principle.[1]

This report presents a completely new design of a reaction calorimeter exploiting a combination of the power compensation and heat balance principles as described by Zogg et al.[4]

The new reaction calorimeter has a volume of 20−50 mL and is equipped with an integrated infrared-attenuated total reflection FTIR ATR probe. Moreover, the new reaction calorimeter is pressure-proof up to 30 bar and needs no calibration. The technical implementation is very different from existing calorimeters.

A metal jacket is used instead of a glass device. This principle is very attractive for small-scale reaction calorimeters because of the simplicity of its technique, as compared to the conventional heat balance implementations. The metal jacket of the calorimeter is patented.[5]

To improve the information content of a single measurement of a reaction, calorimeters are often further combined with analytical sensors such as an IR-ATR probe. Normally IR-ATR probes are quite big,[6,7] and therefore the reaction calorimeters that are equipped with a spectrophotometric sensor require a large volume of 200−2000 mL. Consequently, a significant amount of test substance is needed in a single experiment, which limits application in the development of new pharmaceutical and fine chemicals.

A key aspect of the following applications is the isothermal control of the reaction temperature. This is required for the following three reasons: (1) IR spectra can change as a function of temperature. (2) Kinetic evaluation of the nonisothermal reaction runs implies more unknown parameters than isothermal evaluation. (3) Calorimetric evaluation of nonisothermal data requires the knowledge of the dynamic behavior of the calorimeter.

The new calorimeter has been tested using three chemical reactions: the neutralization of sodium hydroxide with sulfuric acid, the hydrolysis of acetic anhydride, and the acetylation of a substituted benzopyranol (the substrate is not specified because of industry cooperation). The comparison of the results with those of a previous device (CRC.v3) demonstrates the increased precision of the new calorimeter and highlights the fact that the equipment can

* Corresponding author. E-mail: konrad.hungerbuehler@chem.ethz.ch. Telephone: +41 1 632 60 98. Fax: +41 1 632 11 89.

(1) Zogg, A.; Stoessel, F.; Fischer, U.; Hungerbühler, K. Isothermal Reaction Calorimetry as a Tool for Kinetic Analysis. *Thermochim. Acta* **2004**, in press.

(2) Pastré, J.; Zogg, A.; Fischer, U.; Hungerbühler, K. Determination of Reaction Parameters Using a Small Calorimeter with an Integrated FT-IR Probe and Parameter Fitting. *Org. Process Res. Dev.* **2001**, *5*, 158.

(3) Regenass, W. The Development of Stirred Tank Heat Flow Calorimetry as a Tool for Process Optimization and Process Safety. *Chimia.* **1997**, *51*, 189.

(4) Zogg, A.; Fischer, U.; Hungerbuehler, K. A New Small-Scale Reaction Calorimeter That Combines the Principles of Power Compensation and Heat Balance. *Ind. Eng. Chem. Res.* **2003**, *42*, 767.

(5) Hungerbühler, K.; Zogg, A.; Fischer, U. Patent No. EP 1184649, Application No. 00810797.1, 2000.

(6) ASI Applied Systems, ReactIR4000, http://www.asirxn.com/ (Mettler, Toledo).

(7) Bruker, http:\\www.brukeroptics.com.

10.1021/op049900g CCC: $27.50
Published on Web 08/12/2004

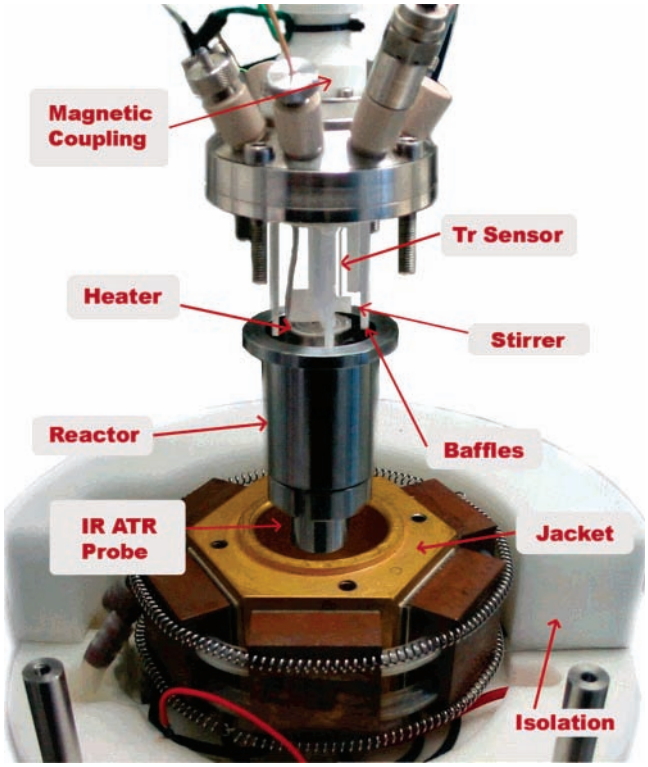

Figure 1. **Overview of the new calorimeter (CRC.v4).**

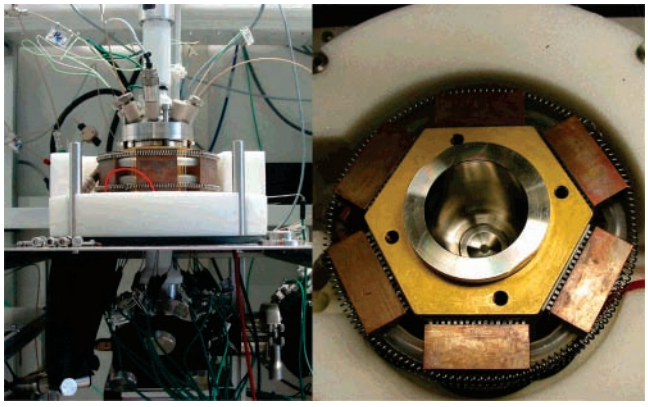

Figure 2. **Front side view of the calorimeter/FTIR system on the left and the top view of the open reactor with the IR-ATR window at the bottom on the right (CRC.v4).**

easily deal with fast and highly exothermic reactions under strictly isothermal conditions.

Equipment

As Figures 1 and 2 show, the new calorimeter (CRC.v4) has been completely redesigned. A preliminary comparison between CRC.v4 and CRC.v3[4] is presented in Table 1. Since in the previous design (CRC.v3) it was not possible to fit the IR-ATR probe from the bottom or through the lid, it was fitted on the lateral cylindrical surface. A design of this type disturbs the cylindrical symmetry of the calorimeter and causes mechanical problems of fixing the probe. The CRC.v4, on the contrary, has a fully symmetrical design. This allows to position the Peltier elements regularly around the reactor and the heat to be uniformly distributed in the jacket. In this way the metal jacket is surrounded with six

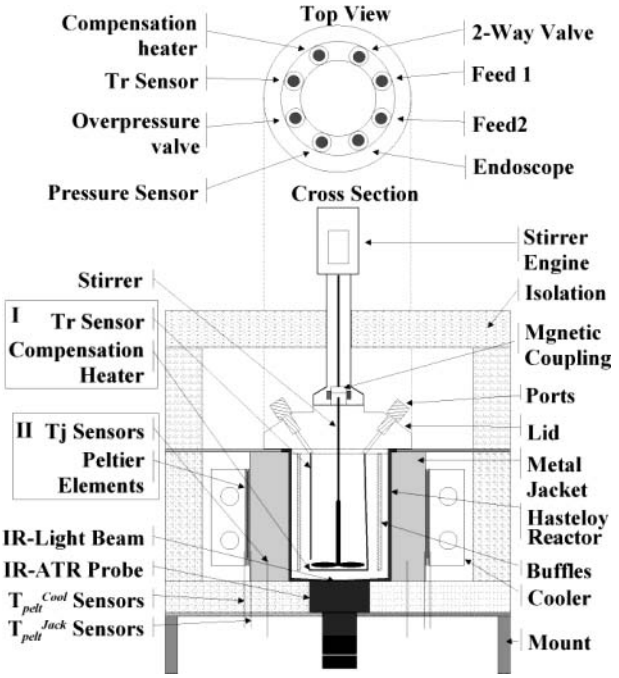

Figure 3. **(CRC.v4): Top view and cross section of the new calorimeter. I: Elements for the power compensation measurement. II: Elements for the heat balance measurement. The eight different inserts are described in the top view. See text for an explanation of the different temperature measurements.**

Peltier elements (Figures 1 and 2), reducing the free jacket surface that can cause heat loss.

The new Hastelloy interchangeable vessel has a diameter of 40 mm and a height of approximately 50 mm. The stand-alone IR-ATR probe by ASI Applied Systems[6] (Figure 2) is fixed to its bottom.

The reaction mixture is stirred by a magnetically coupled stirrer, while the pressure of the reactor and reservoirs (to determine the gas consumption) are measured online.

The heat pumped per unit time by the Peltier elements is 3 times larger compared to that by CRC.v3 due to the six Peltier elements located on the outer surface of the hexagonal prism jacket. The coolers (Figure 3) are connected to a cryostat (Huber CC150) using a mixture of water and alcohol that allows a cooling temperature of −30 °C (T_{cry}) to be reached.

As mentioned in the previous publication[4] the use of a metal jacket instead of a conventional construction with circulating fluid avoids the measurement of the often very small temperature differences between the inlet and outlet stream. On the contrary, with the present design it is possible to measure online the change of q_{Flow} (Figure 4).

The symmetric jacket is monitored by 18 thermocouples. One on each side of the hexagonal prism body to measure the temperature of the metal jacket, six to measure the temperature of the internal face of the Peltier elements, and the last six to measure the temperature of the external face of the Peltier elements which are in contact with the cooling elements.

Since special high-temperature Peltier elements are installed, the maximum jacket temperature is about 200 °C,

Table 1. **Comparison of the main design characteristics of the two calorimeters CRC.v3 and CRC.v4**

	CRC v.4	CRC v.3
Symmetry of the jacket	Yes (hexagonal)	NO
N° of Peltier elements	6	2
N° of thermocouples of the jacket	6 (symmetric)	6 (not symmetric)
N° of thermocouples of the cooler	6	2
N° of thermocouples of the Peltier elem.	6	2
Pressure resistant	Yes (30bar)	No
Connections and connectors	8 { - Power compensation - Temp. sensor - Pressure sensor - Rupture disk - 2 Feed - Sampling pos. - Endoscope } The tubes are made in PEEK	8 { - Power compensation - Temp. sensor - Pressure sensor - Rupture disk - 2 Feed - Sampling pos. - Endoscope } The tubes are made in Teflon
Material of the reactor	Hastelloy	Teflon
Interchangeable reactor	Yes	No
IR-ATR probe	Yes free from the reactor; The optical window is at the bottom of the reactor (Fig. 2);	Yes Direct insert in the reactor, fixed at the sidewall;
Time constant **Compensation heater**	4 sec	4 sec
Peltier elements	15 sec	45 sec
Operating temperature range (T_r in °C)	-20 / +200	-20 / +200
Maximum reaction power	3 kW/L	2 kW/L

and the minimum temperature depends only on the cryostat used. Consequently for the described configuration of CRC.v4 the practical range of the working temperatures is between −20 and 200 °C.

The reactor is supplied with eight inserts (Figure 3), two of these are for feed streams and one to provide samples of the reaction mixture for external analysis (GC, GC/MS, ...). Moreover it is possible to introduce optionally an endoscope to enable visual observations.

The ATR probe is connected to a Mettler Toledo FTIR spectrophotometer (IR4000).[6,8] The spectra of the hydrolysis of acetic anhydride have been recorded with a resolution of 4 cm^{-1} between 600 and 4000 cm^{-1} and a sampling time of 11 s. The dosing of the feed was done using a Jasco pump. The feed temperature (T_{Dos}) is measured by an additional thermocouple placed inside the feed tube. All connection tubes are made of PEEK (polyetheretherketone).[9]

The reactor and all the peripheries are controlled by *LabVIEW*, v6.1 program by National Instruments.[10] The same program is used for the acquisition of the raw data. The sampling rate of the data acquisition and the relative update of the output channel is 10 Hz with a sampling time of 0.1 s. All the data are filtered in *MATLAB* v. 6.5.1 R.13 program by MathWorks[11] using a Butterworth low-pass filter. The measurement data for the Peltier elements are time-corrected using the "Output-Error" model of the MATLAB "ident" toolbox.

(8) Mettler Toledo, http:\\www.mt.com.
(9) Wang, YZ.; Lin, CH.; Chan, BW.; et al. Synthesis and Properties of Thio-Containing Poly(Ether Ether Ketone)s. *Polym. Int.* **2004**, *53*, 320.
(10) *LabVIEW*, v. 6.1; National Instruments, http:\\www.labview.com.

Principle of the Calorimeter

The measurement principle was described by Zogg et al.[4] in detail, therefore only a short overview will be presented here.

The isothermal reaction calorimeter is characterized by two main control loops: A first fast PID (proportional-integral-derivative) loop controls the temperature of the reactor content (T_r) at a constant value by varying the power of the compensation heater.[1] A second slower PID loop controls the temperature of the metal jacket (T_j) at a constant temperature by varying the power of the Peltier elements.

The heat flow balances to be considered in this device are the inner and outer heat balance as indicated in Figure 4. The equations quoted in the following text and the symbols are summarized in Tables 2 and 3.

The inner heat balance is defined in the steady state by eq 1, (the stirrer energy is neglected because it is below the detection limit (0.05 W)). The arrows (Figure 4) show the direction of the heat flow.

$$q^{tot}_{React} = q_{Flow} - q_{Comp} + q_{Lid} - q_{Dos} \quad (1)$$

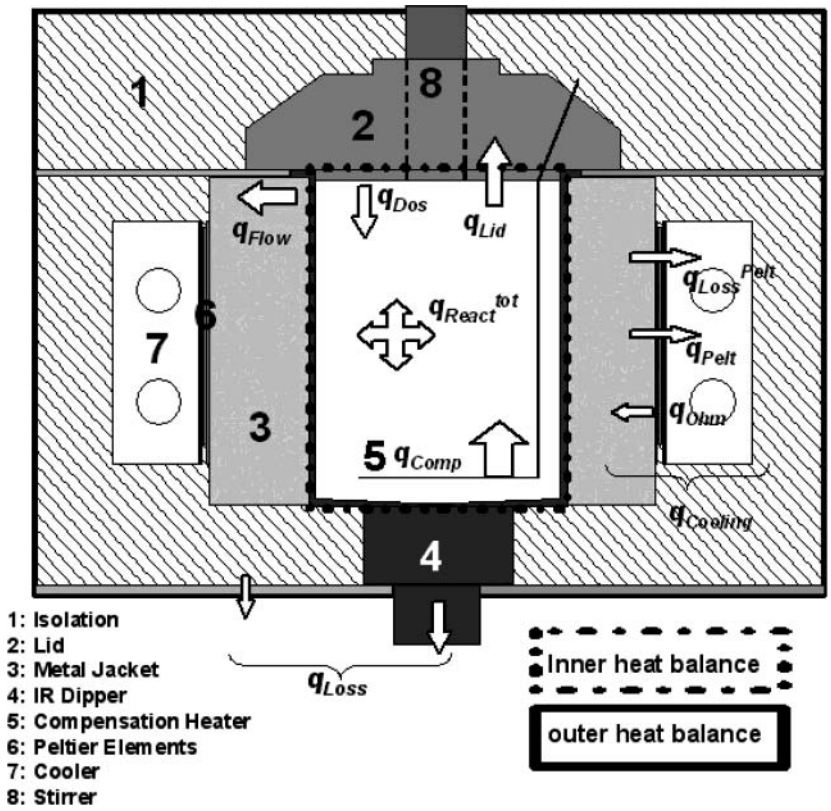

Figure 4. **Heat flow inside the new reactor (CRC.v4). See text for an explanation of the different heat flows.**

Table 2. **Compilation of equations**

terms	equations	no.
q^{tot}_{React}	$q_{Flow} - q_{Comp} + q_{Lid} - q_{Dos}$	(1)
$q_{Cooling}$	$q_{Flow} + q_{Lid} - q_{Loss}$, $q_{Pelt} - q_{Ohm} + q^{Pelt}_{Loss}$, $-SI_{Pelt}T^{up}_{Pelt} - (1/2)RI^2_{Pelt} + K(T^{up}_{Pelt} - T^{down}_{Pelt})$	(2)
q^{tot}_{React}	$q_{Cooling} + q_{Loss} - q_{comp} - q_{Dos}$	(3)
q_{Loss}	$k_{Loss}(T_r - T_{Env})$	(4)
q_{Loss}	$q^0_{Comp} - q^0_{Cooling} + k_{Loss}(\lvert T_r - T_{Env}\rvert - \lvert T^0_r - T^0_{Env}\rvert)$	(5)
$q_{Re\ act}$	$rV(-\Delta_r H)$	(6)
q_{Flow}	$UA(T_r - T_j)$	(7)
q_{Comp}	$I_{Comp} \cdot V_{Comp}$	(8)
q_{Dos}	$fc_p(T_{Dos} - T_r)$	(9)
q_{pelt}	$-SI_{Pelt}T^{up}_{Pelt}$	(10)
q_{Ohm}	$(1/2)RI^2_{Pelt}$	(11)
q^{Pelt}_{Loss}	$k(T^{up}_{Pelt} - T^{down}_{Pelt})$	(12)
S	$a_S((T^{up}_{Pelt} - T^{d}_{Pelt}own/2)) + b_S$, $(V_{Pelt}(I^0_{Pelt})/T^{up}_{Pelt} - T^{down}_{Pelt})$	(13)
R	$\alpha_R(T^{up}_{Pelt} - T^{down}_{Pelt}/2)) + b_R$, $(V_{Pelt}/I_{Pelt}) - S(T^{up}_{Pelt} - T^{down}_{Pelt})/I_{Pelt})$	(14)
K	$\alpha_K((T^{up}_{Pelt} - T_{Pelt}{}^{down}/2)) + b_K$	(15)
k_{Loss}	$k_{Loss,a}(T^0_r - T^0_{Env})^2 + k_{Loss,b}(T^0_r - T^0_{Env}) + k_{Loss,c}$	(16)
$-(\text{d}c_{AcOAc}/\text{d}t)$	$(k' + k''c_{H^+})c_{AcOAc}$, kc_{AcOAc}	(17)
$\text{d}V_r/\text{d}t)$	v_{Dos}	(18)
$\Delta_r H$	$\min_{\Delta_r H}\{\sum_{i=1}^{n}[n_{AcOAc}k(-\Delta_r H) - q^{tot}_{\text{React}i}]^2\}$	(19)

The change of q^{tot}_{React} is balanced by the compensation heater by fast changes of q_{Comp} to keep T_r at the desired level.

The outer heat balance is defined by eq 2:

$$q_{Cooling} = q_{Flow} + q_{Lid} - q_{Loss} \tag{2}$$

The change of $q_{Cooling}$ is compensated by the Peltier elements that vary their power to keep the temperature of the metal jacket T_j at a desired value.

The difference between these two heat balances gives the eq 3:

$$q^{tot}_{\text{React}} = q_{Cooling} + q_{Loss} - q_{Comp} - q_{Dos} \tag{3}$$

Since q_{Comp} and q_{Dos} are measured online the only remaining

(11) *MatLab*, v. 6.5.1 R. 13; MathWorks, http:\\www.mathworks.com.

Table 3. Definitions

symbol	unit	description
A	m^2	total heat-transfer area of the reactor wall
A_{AcOAc}	cm^{-1}	absorbance of acetic anhydride
A_{AcOAc}^{final}	cm^{-1}	absorbance of the acetic anhydride at the end of the reaction
k	W/K	heat conduction coefficient of the Peltier elements
ΔH	J/mol	total measured enthalpy, including the reaction enthalpy $\Delta_r H$ and the heat of mixing Q_{mix} and an eventual heat of phase change Q_{phase}
$\Delta_r H$	J/mol	total reaction enthalpy (first and second reaction enthalpy for a consecutive reaction)
C_{AcOAcA}	mol/L	concentration of acetic anhydride determined on the basis of the IR measurement data
C_{AcOAc}^{C}	mol/L	concentration of acetic anhydride determined on the basis of the thermal measurement data
C_{Dos}	mol/L	concentration of acetic anhydride in the feed
c_p	J/(mol·K)	heat capacity of the reaction mixture
f	mol s^{-1}	feed rate
I_{Comp}	A	current of the compensation heater
I_{Pelt}	A	current of the Peltier elements
I_{pelt}^0	A	current of the Peltier elements before the start of a reaction
K	W/K	heat conduction coefficient through the Peltier elements
k_{Loss}	W/K	empiric proportional coefficient for the calculation of q_{Loss} (it does not depend on the reaction conditions)
$n_{a,b,c...}$	mol	number of moles (of components A, B, C ...)
q	W	heat flow
q_{Comp}	W	power consumption of the compensation heater
	q_{Comp}^0 W	power consumption of the compensation heater before the start of a reaction
$q_{Cooling}$	W	total cooling power of the Peltier elements
$q_{Cooling}{}^0$	W	total cooling power of the Peltier elements before the start of a reaction
q_{Dos}	W	heat flow caused by the dosing of a liquid into the reaction mixture
q_{flow}	W	heat flow from the reactor content through the reactor wall into the reactor jacket
q_{Lid}	W	heat flow from the reactor content through the reactor lid
q_{Loss}	W	heat loss to the environment
q_{Loss}^0	W	heat losses to the environment before the start of a reaction
q_{Loss}^{Pelt}	W	heat flow caused by the passive thermal conduction of the Peltier elements
Q_{mix}	J/mol	heat of mixing
q_{Ohm}	W	heat flow caused by the electrical resistance of the Peltier elements
q_{Pelt}	W	heat flow caused by the Peltier effect
Q_{phase}	J/mol	heat of phase changes
$q_{\mathrm{Re}\ act}$	W	reaction power
q_{Stirr}	W	heat flow caused by the stirring of the reaction mixture
q_{Stirr}^0	W	heat flow caused by the stirrer before the start of a reaction
$q_{\mathrm{Re}act}^{tot}$	W	total power consumption or production during a reaction measurement (it contains the reaction power $q_{\mathrm{Re}\ act}$ and any other thermally active processes such as heat of mixing (q_{mix}) or heat of phase change (q_{phase}))
r	mol/(L·s)	reaction rate
R	J/(mol·K)	ideal gas constant
R	W	electrical resistance of the Peltier elements
S	V/K	Seebeck coefficient of the two Peltier elements in series
T_{Cry}	K	temperature of the cryostat
T_{Env}	K	temperature of the environment
T_{Env}^0	K	temperature of the environment before the start of a reaction
T_{Dos}	K	temperature of the dosed liquid
T_{Pelt}^{down}	K	temperature of the thermocouple used to measure cold-side temperature of the Peltier elements
T_{Pelt}^{up}	K	temperature of the thermocouple used to measure hot-side temperature of the Peltier elements
T_j	K	jacket temperature
T_j^0	K	jacket temperature before the start of a reaction
T_r	K	reaction temperature
T_r^0	K	reaction temperature before the start of a reaction
V_{Comp}	V	voltage of the compensation heater
V_{Comp}	V	voltage of the Peltier elements
V_{Dos}	L/s	dosing rate
V_r	L	reactor volume
U	W/(m^2·K)	overall heat-transfer coefficient

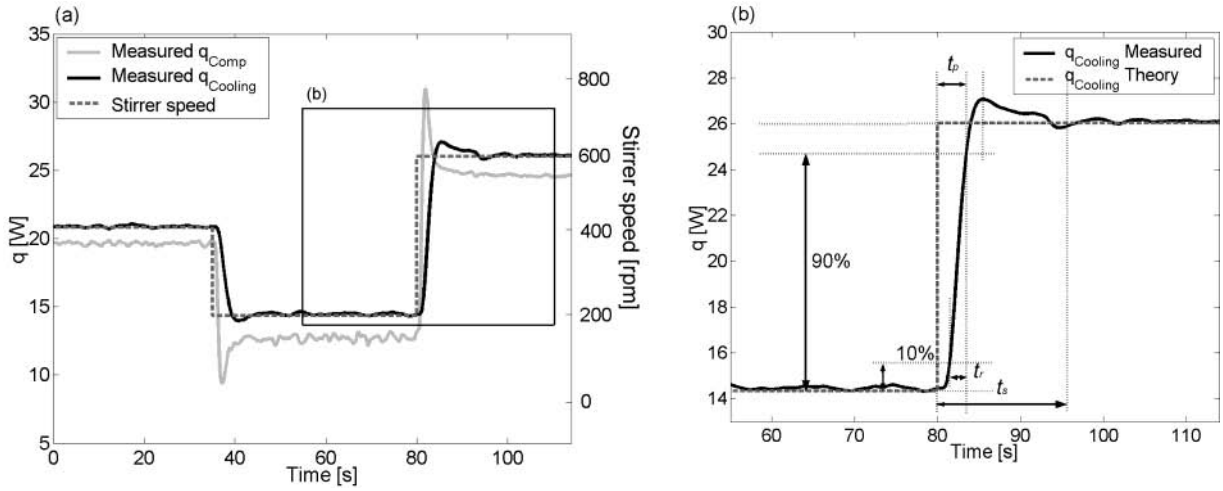

Figure 5. **CRC.v4: (a) Heat flow measurement of $q_{cooling}$ and q_{Comp} (b) Heat flow measurement of $q_{cooling}$, at $T_r = 25$ °C when a steplike change in the stirrer speed has to be compensated. t_r is the time until the signal has increased from 10% to 90%, t_p is the time between the stirrer change and the maximum peak of the signal, and t_s is the time to reach the steady state.**

unknowns in this combined heat balance are q_{Loss}, the heat loss through the isolation and via the conductivity of the inserts (eqs 4 and 5, Table 2), as well as the total amount of heat pumped by the Peltier elements ($q_{Cooling}$) that comprises three different heat flows[12] (eqs 2, 10−12, Table 2). The determination of the parameters of the Peltier elements is described by Zogg et al.[4]

Therefore, by measuring two independent control loops with two independent heat signals ($q_{Cooling}$ and q_{Comp}, see eqs 2 and 8, Table 2) any change of the baseline can be distinguished from the reaction power. This means that neither a mathematical baseline correction nor a calibration of the value *UA* (eq 7, Table 2) is required.

Characterization of the Time Constant of the Calorimeter. A small-scale calorimeter must be able to measure rapid and highly exothermic reactions correctly, and this demands a fast-responding control system.

Figures 5 and 6 can be analyzed to characterize the time constants of the new calorimeter.

To do this in a first experiment (Figure 5), the calorimeter was charged with water and thermostated at 25 °C (±0.01 °C). During this state the stirrer speed was shifted from 400 to 200 and to 600 rpm to change the overall heat-transfer coefficient and by this the heat flow through the wall (eq 7, Table 2).

The time constants of the power signals (q_{Comp} and $q_{Cooling}$; note the high parallelism of the two signals in case of no reaction according to eq 3, Table 2) are now determined by measuring the response of the instrument to the instantaneous change of the inner heat resistance by the above-described profile of the stirrer speed. This thermal response signal now allows the characterization of the time constant τ by the time delays t_r, t_p, and t_s, where t_r is the time until the signal has increased from 10 to 90%, t_p is the time between the stirrer speed change and the maximum peak of the signal, and t_s is the time to reach the steady state (Figure 5a), according to the following equation[13,14]

$$\tau = \frac{t_p\sqrt{1-\xi^2}}{\pi} \quad \text{with} \quad \xi = \frac{2.3 \cdot t_r}{0.9 \cdot t_s}$$

The data from Figure 5 give a response time for q_{Comp} of about 4 s and for $q_{Cooling}$ of about 15 s.

For standard reaction calorimeters time constants are reported in the range of 50 s[15] to 85 s. For CPA 200 by Chemisens[16] (max 250 mL) a time constant of about 50 s is reported. The high precision calorimeter C80 (12.5 mL,

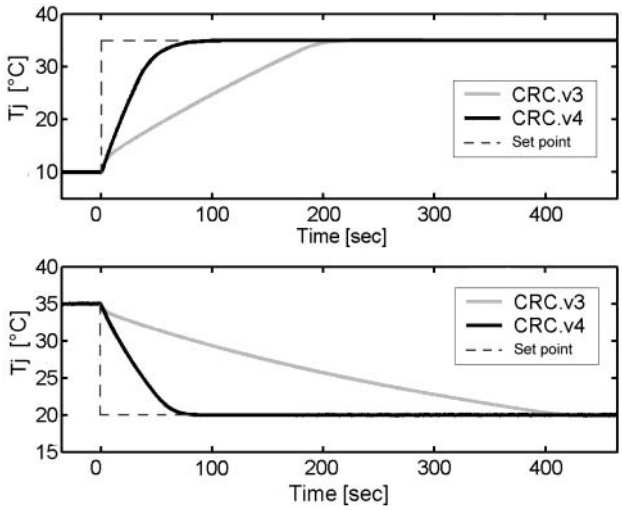

Figure 6. **CRC.v4 and CRC.v3 comparison of the dynamic behaviour of the jacket temperature (T_j). (a) Increasing the set point of T_j from 10 to 35 °C. (b) Decreasing the set point of T_j from 35 to 20 °C.**

(12) Nilsson, B. J.; Silvegren, C.; Törnell, B. A Calorimetric Investigation of Suspension and Emulsion Polymerization of Vinyl Chloride. *Angew. Makromol. Chem.* **1983**, *112*, 125.

(13) Zogg, A. A Combined Approach using Calorimetry and IR-ATR Spectroscopy for the Determination of Kinetic and Thermodynamic Reaction Parameters. Dissertation ETH Nr. 15086. 2003.

(14) Franklin, G. F.; Powell, J. D.; Emami-Naeini, A. *Feedback Control of Dynamic Systems*, 4th ed.; Prentice Hall: Reading, 2002.

(15) Riesen, R.; Grob, B. Reaktionskalorimetrie in der Chemischen Prozessentwicklung. *Swiss Chem.* **1985**, *7*, 39.

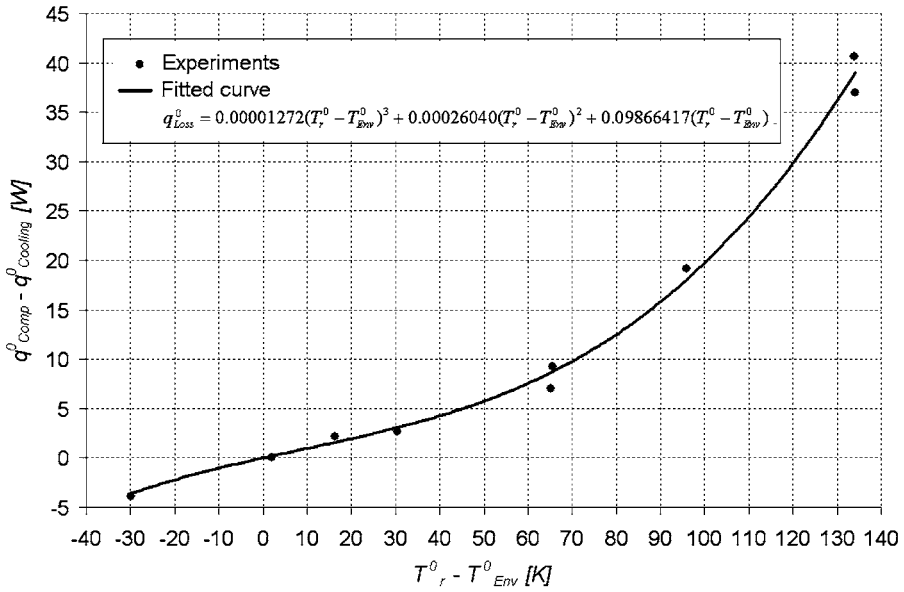

Figure 7. **Calibration curve of CRC.v4 for the characterization of q_{Loss}.**

Setaram[17]) has a time constant of about 170 s. On the contrary, the time constant for the power compensation signal (q_{comp}) of the CRC.v3 is the same as for the CRC.v4 (4 s), whereas the signal of the Peltier elements ($q_{Cooling}$) reacts within about 45 s for the CRC.v3 (Table 1). This different behavior of the heat balance signal is mainly caused by the different thermal behavior of the copper block used as a reactor jacket (with six instead of two Peltier elements) and by the different construction materials of the vessel (Hastelloy versus Teflon). This difference can be also seen in a second dynamic experiment when the set point of T_j has been changed from 10 to 35 °C (Figure 6a) and from 35 to 20 °C (Figure 6b).

Characterization of q_{Loss}. The heat flow q_{Loss} represents the heat loss though the isolation and via conductivity of inserts (dosing, stirrer, etc.). Because q_{Loss} is independent of the reactor content, it is easier to describe than q_{Flow}.[13] The standard way to calculate q_{Loss} is to postulate a proportionality to the driving temperature force:[18]

$$q_{Loss} = k_{Loss}(T_r - T_{Env}) \tag{4}$$

The coefficient k_{Loss} is a device specific parameter and is again independent from the reactor content, the stirrer speed, and the viscosity. Calibrating the calorimeter k_{Loss} has to be determined only once as the thermal insulation of the reactor is well defined and does not change during the experiments.

The calibration was done varying the reactor temperature in a range between −5 and +160 °C (Figure 7). The calorimeter was charged with water for the experiments at T_r = 25, 40, 55, 90 °C and with a silicon oil for the experiments at T_r = −5, 90, 120, 160 °C and thermostated at the desired temperature level.

Since in the calibration experiments there is no dosing or reaction, q^0_{Loss} can be written according to eqs 3 and 4:

$$q_{Loss}{}^0 = q_{Comp}{}^0 - q_{Cooling}{}^0 = k_{Loss}(T_r{}^0 - T_{Env}{}^0)$$

After reaching steady state q^0_{Loss} can be calculated by the difference between $q^0_{Comp} - q^0_{Cooling}$.

A third degree polynomial function for q^0_{Loss} was fit to the experimental points to get the calibration curve for the temperature range measured (eqs 4 and 16, Table 2). The values of $k_{Loss,a}$, $k_{Loss,b}$, and $k_{Loss,c}$ from Figure 7 are now used for all the following calculations. As it can be seen from Figure 7, the temperature sensitivity of q_{Loss} (slope) increases with higher temperature. This has the consequence of lower accuracy for high-temperature measurements (T_r > 100 °C).

Because the reactor is isolated (Figures 1−4), the heat loss to the surroundings can be assumed to be constant during a reaction. This assumption is feasible as long as the temperature of the environment (T_{Env}) does not change significantly. However, it is more accurate to include T_{Env} into the heat flow balance. Therefore, the following relationship between q_{Loss} and T_{Env} is used according to Zogg:[4]

$$q_{Loss} = q_{Comp}{}^0 - q_{Cooling}{}^0 + k_{Loss}(|T_r - T_{Env}| - |T_r{}^0 - T_{Env}{}^0|) \tag{5}$$

All heat flows that remain in the combined heat flow balance (eq 3, Table 2) are finally represented by measured values.

Reaction Experiments

For testing the reactor and to compare the results of CRC.v4 and CRC.v3 we chose two well-known chemical reactions: neutralization of NaOH and hydrolysis of acetic anhydride.

The acetylation experiment that caused some problems in CRC.v3 is added.

Neutralization of NaOH with H_2SO_4.

$$2NaOH + H_2SO_4 \rightarrow Na_2SO_4 + 2H_2O$$

The reactor was filled in a first step with 26 mL of 2.77 N NaOH (Titrisol, Merck). The stirrer speed was turned on

(16) Christensen, J. J.; Gardner, J. W.; Eatough, D. J.; Izatt, R. M. An Isothermal Titration Microcalorimeter. *Rev.Sci. Instrum.* **1973**, *44*, 481.
(17) Setaram, http:\\www.setaram.com.
(18) Hemminger, W.; Höhne, G. *Calorimetry Fundamentals and Practice*; Weinheim: Deerfield Beach, Florida and Basel.

to 600 rpm, and the reaction temperature T_r was set to 25 °C. In a second step 14.4 mL of 4 N H_2SO_4 (Fluka) was added at 3.6 mL/min in the reactor. The experiment was repeated three times. To determine q_{Dos} the heat capacity of the feed mixture (3.61 kJ/kg·K) was taken from Landolt−Börnstein.[19]

Hydrolysis of Acetic Anhydride.
After having measured the reference background spectrum

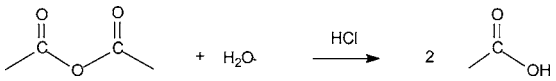

for the IR spectrophotometer the reactor was filled with 35 mL of HCl 0.1 N (Titrisol, Merck). The stirrer speed was turned on to 600 rpm, and the reaction temperature T_r was set. Then 2 g of a mixture of 10.72 mmol of acetic anhydride (Fluka) and 15.12 mmol of acetic acid (Sharlau) was added with a constant dosing rate of 5 mL/min. The experiments were carried out at three reaction temperature levels T_r = 25, 40 and 55 °C three times. To determine q_{Dos}, the heat capacity of the feed mixture (1.83 kJ/kg·K) was calculated using the mass fraction and the heat capacities of the pure components (acetic anhydride: c_p = 1.65 kJ/kg·K and acetic acid: c_p = 2.05 kJ/kg·K).[19]

Acetylation of a Substituted Benzopyranol.
At the beginning of each acetylation experiment the empty

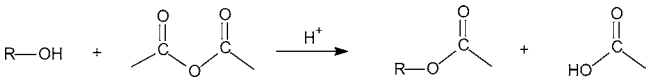

reactor was purged with N_2, and a reference background spectrum for the IR spectrophotometer was measured. In a second step a mixture of 22 mL of the substitute benzopyranol and 5 mL of acetic anhydride was added to the reactor. The stirrer speed was set to 600 rpm and the reactor temperature T_r to 60 °C. In a third step 0.3 mL of a mixture of 0.15 mmol of acetic anhydride (Fluka) and 0.05 mmol of sulphuric acid (Fluka 98%) was added with a constant dosing rate of 0.5 mL/min. To determine q_{Dos} the heat capacity of the feed mixture (1.58 kJ/kg·K) was calculated using the mass fraction and the heat capacities of the pure components (acetic anhydride: c_p = 1.65 kJ/kg·K and acetic acid: c_p = 2.05 kJ/kg·K).[19] The experiment was carried out three times.

Results and Discussion

Neutralization of NaOH with H_2SO_4. Figure 8 shows the results of the CRC.v4 for the neutralization of the NaOH with H_2SO_4 (results identical to those of CRC.v3[4]).

This very fast reaction provides an example of the change of heat flow through the wall during reaction time. In this case the heat-transfer area A is changing (eq 7, Table 2); the large shift is caused by the dosing of 14.4 mL of H_2SO_4 into 26 mL of NaOH (change of A of about 55%).

As shown by Zogg et al.,[4] if only the power compensation signal would be available as in the case of conventional calorimeters, this baseline change would have to be compensated mathematically by supposing a linear change of the heat-transfer area (UA). With the new calorimeter, this mathematical correction is no longer needed because the q_{Comp} signal is compensated by the heat balance measurement $q_{Cooling}$. The q^{tot}_{React} is calculated therefore without any calibration or correction of the heat-transfer coefficient (eq 3, Table 2).

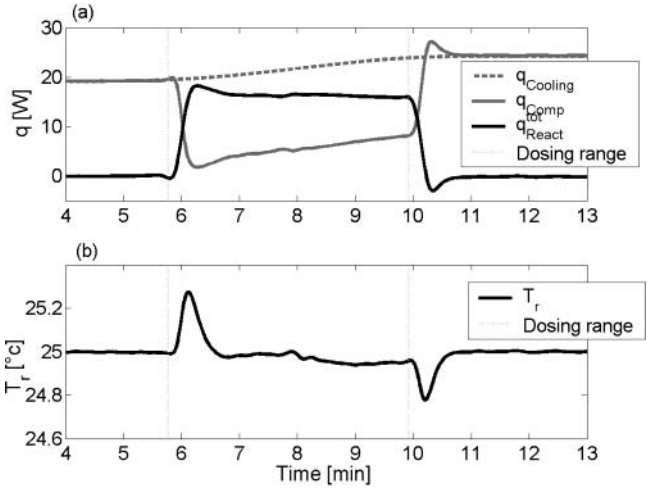

Figure 8. **(CRC.v4): Neutralization experiment of NaOH with H_2SO_4 at 25 °C. (a) For the heat flow signal the maximum power of the reaction is about 550 W/L. The changing baseline of the q_{comp} signal is mainly caused by the change of the heat-transfer area due to the volume increase from the dosing of the H_2SO_4. (b) The precision of the reaction temperature control. The dosing period is indicated with the vertical lines.**

The integration of the q^{tot}_{React} gives a reaction enthalpy of −134 ± 2 kJ/mol (mol of H_2SO_4), which is close to the literature values of −134,[4,17] −132,[19] and −139.1[20] kJ/mol. Figure 8b also shows the precision of the reaction temperature control. The maximum reaction power of about 550 W/L is removed rapidly; as it can be seen from the T_r curve, the temperature of the reactor content is only changing by 0.3 K over a short period of about 40 s at the beginning and at the end of the dosing period.

Hydrolysis of Acetic Anhydride. Figure 9 shows the q^{tot}_{React} of the hydrolysis of the acetic anhydride at three different temperature levels (25, 40, and 55 °C) (also here the results are very similar to those of CRC.v3[4]). As can be seen, the deviation from the temperature set point is quite small. The q^{tot}_{React} at 25 °C shows a significant peak at the beginning of the reaction. As reported by Zogg et al.,[4] Becker et al.[21], Köhler et al.,[22] and Maschio et al.[23] this peak corresponds to the heat of mixing during the dosing phase.

(19) Landolt, H.; Börnstein, R.; Hellwege, K. H. *Numerical Data and Functional Relationships in Science and Technology*, 6th ed.; Springer: Berlin, 1987; Vol. 4, Part 4.

(20) Schildknecht, J. Reaction Calorimeter for Applications in Chemical Process Industries: Performance and Calibration. *Thermochim. Acta* **1981**, *49*, 87.

(21) Becker, F.; Walisch, W. Isothermal calorimetry with automatically controlled Peltier-cooling and continuous integration of the compensation power. (Isotherme Kalorimetrie mit automatisch gesteuerter Peltier-Kü hlung und fortlaufender Integration der Kompensationsleistung). *Z. Phys. Chem. Neue Folge.* **1965**, *46*, 279.

(22) Köhler, W.; Riedel, O.; Scherer, H. An isothermal Calorimeter controlled by Heat Pulses. Part II: Examples for Calorimetric and Calorimetric-Kinetic Measurements. (Ein mit Heizimpulsen Gesteuertes Isothermes Kalorimeter. Teil II: Anwendungsbeispiele für Kalorische und Kalorisch-Kinetische Messungen). *Chem.-Ing.-Tech.* **1973**, *22*, 1289.

(23) Ampelli, C.; Di Bella, D.; Lister, D. G.; Maschio, G.; Stassi, A. Study of the Hydrolysis of Acetic Anhydride by Means of a Simple, Low Cost Calorimeter. *Riv. Combust.* **2001**, *55*, 292.

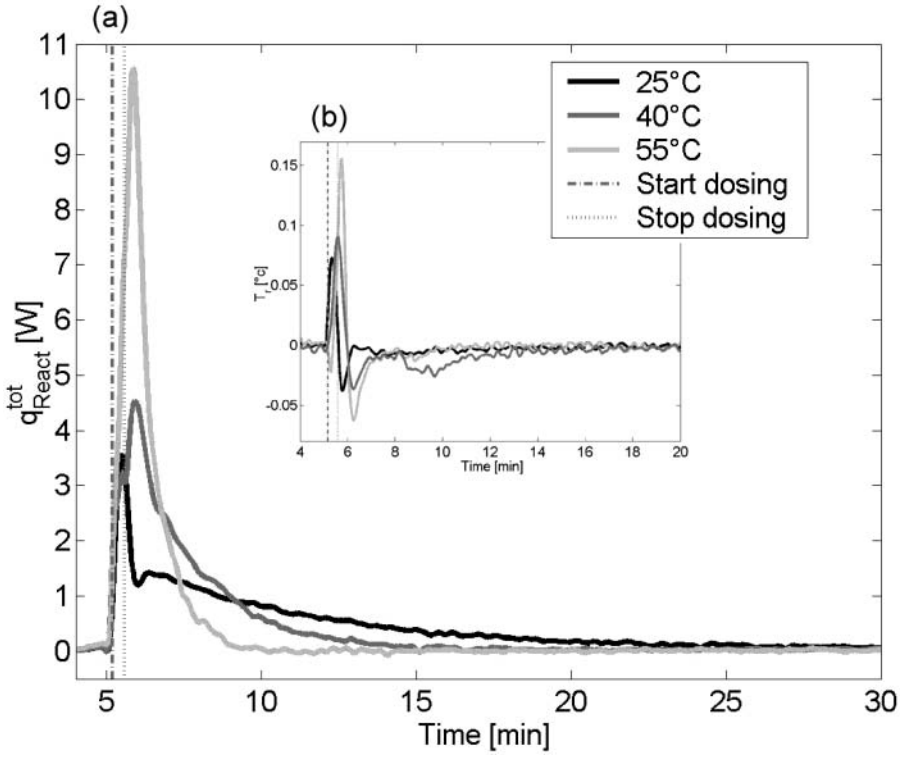

Figure 9. **(CRC.v4): Reaction power (q^{tot}_{React}) (a) and temperature behaviour (b) of the hydrolysis of acetic anhydride measured at 25, 40, and 55 °C.**

Because the reaction is carried out quite diluted in 0.1 M HCl ($c_{H2O} \approx$ const and $c_{H}+ \approx$ const) the reaction kinetics can be assumed to be pseudo-first-order.[21,22] According to eq 17, Table 2 (Zogg et al.,[4,24] Becker,[21,25] and Maschio et al.[23]) one could separate the observed heat of mixing at the beginning of the experiment from the heat of reaction (Figure 10a). $\Delta_r H$ (eq 19, Table 2) and Q_{mix} at 25 °C were measured as -61 ± 2 kJ/mol and -6 kJ/mol which is in good agreement with the literature (Table 4). In a next step the first-order rate constant k was calculated by linear regression using q^{tot}_{React} data. The first-order rate constant at 25 °C was determined to be $2.8 \pm 0.1 \times 10^{-3}$ s^{-1}. This value is also in good agreement with the value of $3.0 \pm 0.2 \times 10^{-3}$ s^{-1} from CRC.v3 and the value of $2.76 \pm 0.06 \times 10^{-3}$ s^{-1} reported by Martin[26] who carried out the experiments under similar conditions in a precursor of RC1 (Table 4). The determination of the enthalpies and the rate constant was repeated at 40 and 55 °C (Table 4).

For the rate constant calculated from q^{tot}_{React} at three temperature levels, the activation energy E_a was determined to be 56 kJ/mol (Figure 11) which is again in good agreement with the CRC.v3 data[4,24] and the literature value of 57 kJ/mol[26] (Table 4).

The hydrolysis reaction was further followed with the integrated IR-ATR probe. To determine the first-order rate constant on the basis of the IR measurements the easiest and most efficient way is to find a wavelength where only one component is absorbing. From this point of view the peak at 1139 cm^{-1} (Figure 12), which corresponds to the C−O−C stretch vibration of acetic anhydride, was chosen.

The plot of Figure 10b shows the decrease of this absorbance of the acetic anhydride (A_{AcOAc}) with time in terms of concentration.

The absorbance data were converted to concentration units using the following equation:

$$C^{A}_{AcOAc} = (A_{AcOAc} - A^{final}_{AcOAc}) \frac{\max(c_{AcOAc})}{\max(A_{AcOAc} - A^{final}_{AcOAc})}$$

As can be seen from Figure 10b, the concentration of acetic anhydride determined on the basis of the IR measurement data (C^{A}_{AcOAc}) and the corresponding concentration of acetic anhydride determined on the basis of the thermal measurement data (C^{C}_{AcOAc}) are in good agreement.

Similar to the thermal evaluation, the reaction rate constant k can also be determined from the C^{A}_{AcOAc} data set by a linear regression. The regression was done for the same time period as was used for the regression of the thermal measurements. The first-order rate constant at 25 °C was determined to be $2.6 \pm 0.1 \times 10^{-3}$ s^{-1} and is in good

(24) Zogg, A.; Fischer, U.; Hungerbühler, K. A New Approach for a Combined Evaluation of Calorimetric and Online Infrared Data to Identify Kinetic and Thermodynamic Parameters of a Chemical Reaction. *Chemom. Intell. Lab. Syst.* **2004**, *71*, 165.
(25) Becker, F.; Maelicke, A. Thermokinetic measurements using the principle of heat-flow calorimetry. (Thermokinetische Messungen nach dem Prinzip der Waïrmeflusskalorimetrie). *Z. Phys. Chem. Neue Folge.* **1967**, *55*, 280.
(26) Martin, H. Wärmeflusskalorimetrie unter präparativen Bedingungen und ihre Anwendung zur Verfolgung der Isomerisierungskinetik von Trimethylphosphit. Ph.D. Thesis, University of Basel, Basel, Switzerland 1975.
(27) André, R.; Boou-Diab, L.; Stoessel, F.; Giornano, M.; Mathonat, C. A New Reaction Calorimeter for Screening Purposes during Process Development. *Org. Process Res. Dev.* **2002**, *6*, 915.
(28) *NIST Chemistry Webbook*; Standard Reference Database Number 69; National Institute of Standards and Technology: Washington, DC, online, 2003.
(29) *CRC Handbook of Chemistry and Physics*, 3rd electronic edition; CRC Press: Boca Raton, FL, 2000.

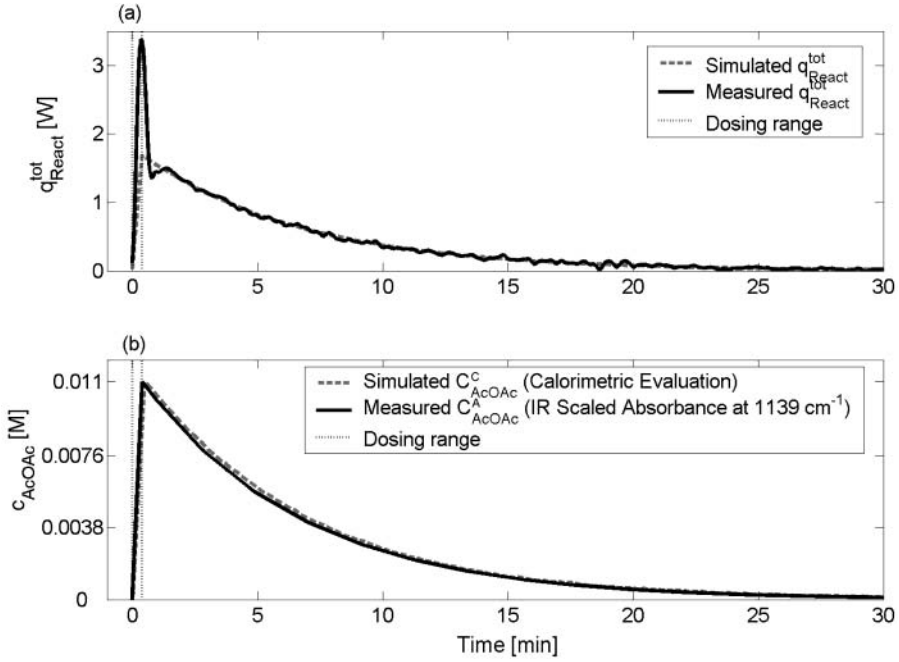

Figure 10. **(CRC.v4): Separated evaluation of the calorimetric (a) and infrared (b) data at $T_r = 25$ °C. (a) Measured and simulated reaction power. (b) Measured and simulated concentration time curve of acetic anhydride simulated with the kinetic parameters obtained from the calorimetric measurement compared to the one determined by the IR measurement at 1139 cm^{-1}.**

Table 4. **Summary of the results for the hydrolysis of acetic anhydride**

	CRC.v4		
	T_r (°C)		
	25	40	55
ΔH [kJ/mol][a]	-61 ± 2	-59.5 ± 2	-58 ± 2
$\Delta_r H$ [kJ/mol][b]	-55 ± 3	-55 ± 1	-55 ± 1
Q_{mix} [kJ/mol][c]	−5.8	−4.5	−3.2
k [10^{-3} s^{-1}] calcd data[d]	2.8 ± 0.1	7.6 ± 0.1	22 ± 0.2
k [10^{-3} s^{-1}] IR data[e]	2.6 ± 0.1	7.4 ± 0.2	21.1 ± 0.2
k [10^{-3} s^{-1}] comb. alg.[f]			
E_a [kJ/mol] calcd data[g]		56	
E_a [kJ/mol] IR data[h]		55	
E_a [kJ/mol] comb. alg.[i]			

	literature						
	T_r (°C)						
	0	10	15	25	35	40	55
ΔH [kJ/mol][a]	−57[22]	−65.9,[23] −58[27]	−63.1,[23] −59[26]	−60,[4] −65,[22] −62,[21,25] −60.4,[23] −61,[26] −58[27]	−58.2,[23] −59[26]	−59,[4] −58.4,[23] −58[27]	−57[4]
$\Delta_r H$ [kJ/mol][b]		−61.9[23]	−60.8[23]	−57,[4,21,25] −60.1,[23] −56,[j] −58[k]	−59.0[23]	−62,[4] −59.8[23]	−60[4]
Q_{mix} [kJ/mol][c]		−4[23]	− 2.3[23]	−3,[4] −5,[21,25] −0.3[23]	+0.9[23]	+3,[4] +1.4[23]	+3[4]
k [10^{-3} s^{-1}] Calcd data[d]		0.8[23]	1.2[23]	3.0 ± 0.2,[4] 2.33[23]	4.47[23]	8.5 ± 0.6,[4] 5.77[23]	23.5 ± 0.8[4]
k [10^{-3} s^{-1}] IR data[e]				2.8 ± 0.2[4]		7.8 ± 0.3[4]	22.2 ± 0.5[4]
k [10^{-3} s^{-1}] comb. alg.[f]				2.8[24]		8.2[24]	21.9[24]
E_a [kJ/mol] dalcd data[g]				57,[4] 57,[21,25] 48.6,[23] 57[26]			
E_a [kJ/mol] IR data[h]				57,[4] 54[24]			
E_a [kJ/mol] comb. alg.[i]				56[24]			

[a] ΔH includes the heat of mixing. [b] $\Delta_r H$ is the heat of reaction assuming a first-order kinetic without heat of mixing. [c] Heat of mixing. [d] First-order rate constant calculated by linear regression of the natural logarithms of q_{React}. [e] First-order rate constant calculated by linear regression of the natural logarithms on the basis of the IR measurements. [f] First-order rate constant calculated with the combined evaluation algorithm by Zogg.[22] [g] Activation energy calculated by linear regression of the natural logarithms of q_{React}. [h] Activation energy calculated by linear regression of the natural logarithms on the basis of the IR measurements. [i] Activation energy calculated with the combined evaluation algorithm by Zogg.[24] [j] Calculation based on tabulated standard enthalpies of formation [NIST].[28] [k] Calculation based on tabulated standard enthalpies of formation [CRC].[29]

agreement with the value determined from the calorimetric measurements ($2.8 \pm 0.1 \times 10^{-3}$ s^{-1}) and from the literature values (Table 4). The determination of the rate constant based on spectroscopic measurement was repeated at 40 and 55 °C (Table 4). Again from these values the activation energy E_a was calculated (Figure 11, IR measurements) to be 55.1

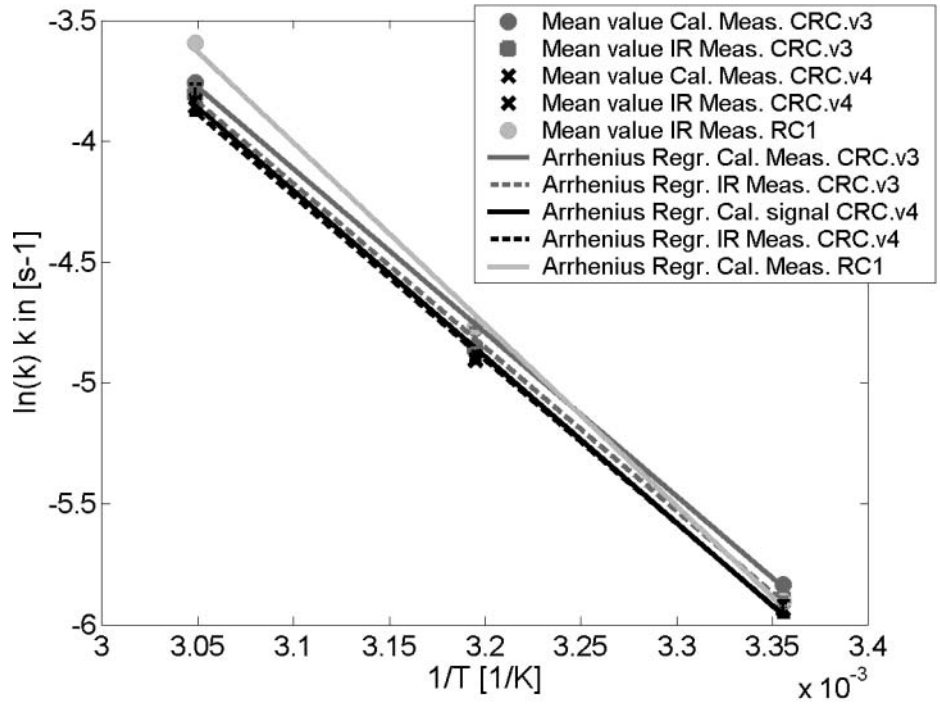

Figure 11. **Arrhenius plots of the determined rate constants of CRC.v4 compared with the data of CRC.v3 and RC1 at 25, 40, 55 °C for the hydrolysis of the acetic anhydride. All the measurement points are the mean value of three identical experiments.**

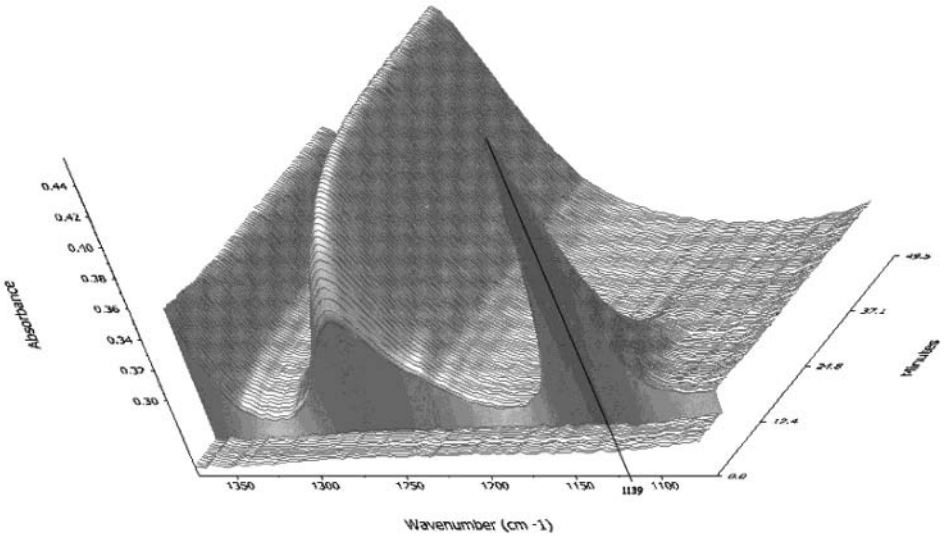

Figure 12. **Part of the IR spectrum recorded as a function of time during a hydrolysis reaction of acetic anhydride at 25 °C. The peak indicated at 1139 cm^{-1} was used to determine the decreasing concentration of acetic anhydride during the hydrolysis (Figure 10b).**

kJ/mol which fits well with the value determined from thethermal measurements (56 kJ/mol) as well as from CRC.v3[4,24] and literature data.[26]

By comparing the measured reaction power q^{tot}_{React} at 25 °C with the measured IR signal (Figure 10), it becomes finally obvious that the initial peak of the q^{tot}_{React} curve is not visible in the IR signal and is therefore not related to the chemical reaction but to the heat of mixing.

Acetylation of a Substituted Benzopyranol. In Figure 13 the reaction power of the acetylation of a substituted benzopyranol is shown, and the signals of three different reaction calorimeters undergoing the same reaction under the same conditions are compared (CRC.v4, CRC.v3, and RC1[8]). As shown in Figure 13(b) CRC.v3 is not able to compensate completely (5% of error); the baseline shift may be due to the change of viscosity during the reaction (from 0.12 to 0.14 kg/m·s). On the contrary the signals of the commercial reaction calorimeter RC1 and of the CRC.v4 are well compensated but with some difference.

This difference can be explained with the help of Figure 14 which shows the comparison of the reactor temperature (T_r) during the reaction in these two calorimeters, CRC.v4 and RC1. It can be seen that the assumed isothermal behaviour is maintained only in the CRC.v4 with 0.55 °C

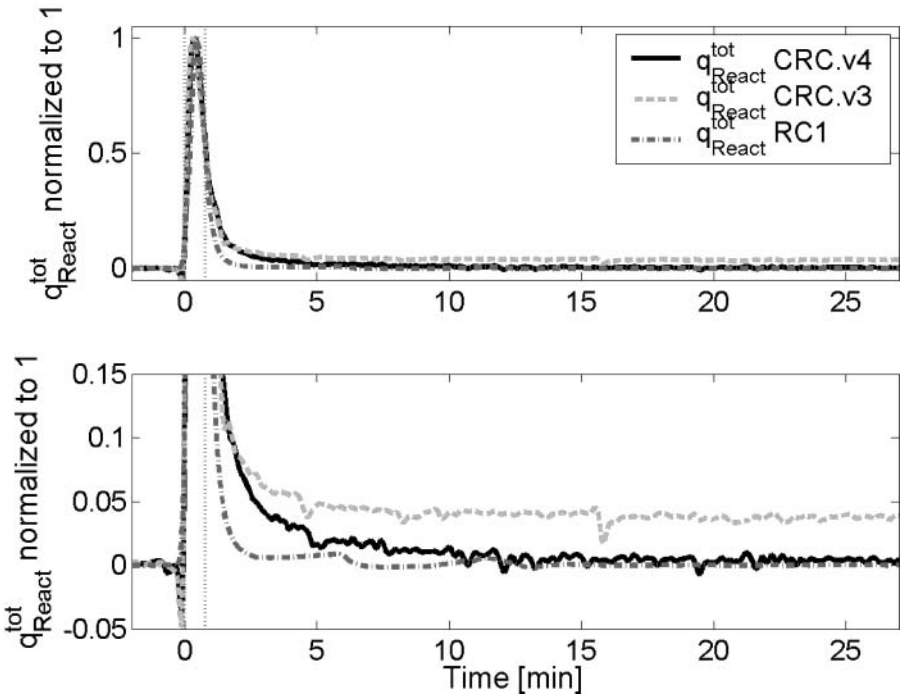

Figure 13. **Signal comparison of CRC.v4/CRC.v3/RC1. (a) Evaluation of the heat of the reaction for the acetylation of a benzopyranol at 60 °C. (b) Zoom of the baseline compensation.**

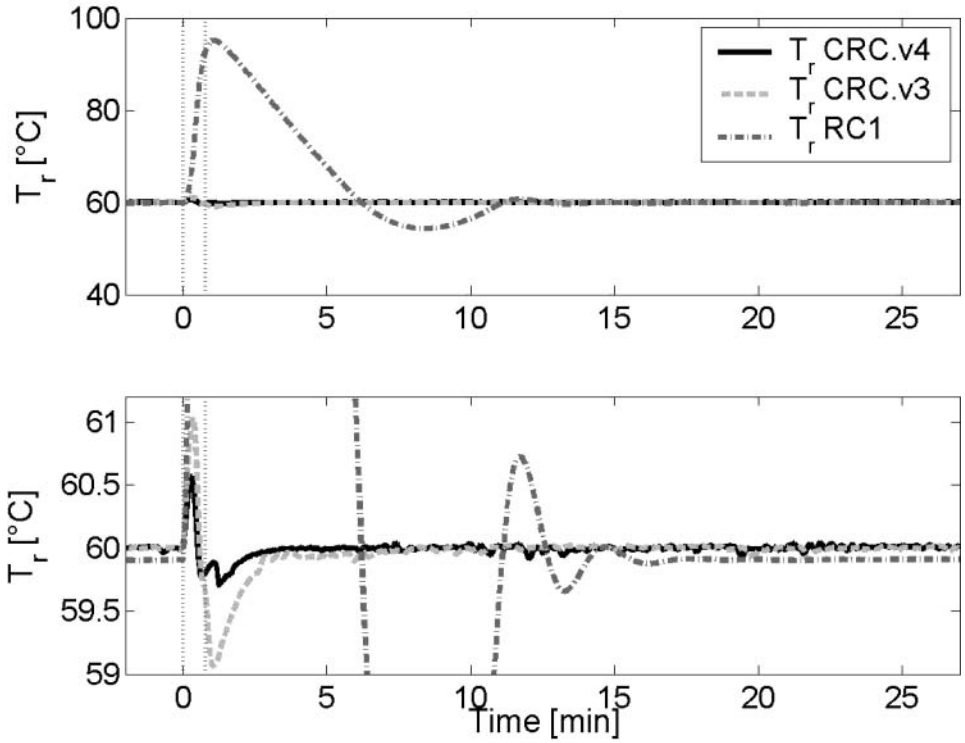

Figure 14. **Difference from set point during the acetylation of a benzopyranol at 60 °C. (a) Comparison of the temperature deviation between CRC.v4, CRC.v3, and RC1(maximum deviation for RC1 35 °C). (b) Zoom of the temperature deviation of the CRC.v4 (maximum deviation of the set point for CRC.v4 = 0.55 °C).**

of deviation from the set-point temperature of the reactor, whereas a temperature deviation up to 35 °C was observed in the RC1 during the reaction time.

The integration of the two signals shows that the $\Delta_r H = -68$ kJ/mol of the RC1 is higher than the $\Delta_r H = -64$ kJ/mol of the CRC.v4. The different enthalpy of the reaction determined by the RC1 can be a consequence of the nonisothermal conditions. Such a temperature deviation would be even much more problematic in the context of a kinetic evaluation.

The results presented demonstrate that the combination of the new Hastelloy vessel with the metal jacket of CRC.v4

is able to maintain isothermal conditions and at the same time to compensate the baseline drift for even very rapid and highly exothermic reactions with significant viscosity changes (Figure 14).

Conclusions and Outlook

To identify the optimal operating conditions of a chemical process, knowledge of kinetic and thermodynamic parameters is required. For this reason the reaction calorimetry technique is used as a standard analytical tool.

The design and performance of a pressure-resistant small-scale reaction calorimeter integrated with an IR-ATR probe was presented. An in situ online correction for the overall heat-transfer coefficient avoids the need of any calibration.

The maximum reaction power that can be determined by CRC.v4 is about 3 kW/L (Table 1). The performance compared with state-of-the-art devices shows remarkable improvements as the short time response and the ability to maintain isothermal conditions at quite extreme reaction conditions. This was demonstrated by the acetylation experiment (Figure 14). The system is able to maintain isothermal conditions and to compensate for the baseline drift even for very fast and highly exothermic reactions with a significant change in viscosity during reaction. Therefore, with the combination of the power compensation and the heat balance principle the error due to the change of the boundary conditions on the wall of the vessel can be reduced. The results of the new device are accurate, reproducible, and in good agreement with the literature data.

A further advantage of the small volume is the potential of connecting several of these calorimeters to the same cryostat. Temperature changes of the cooling liquid do not affect the calorimetric signal because there is the individual control of the jacket temperature by the Peltier elements.

The equipment has a high potential for the study of gas−liquid reactions under pressure. Therefore, three-phase catalytic hydrogenations will build the next extension of our reaction calorimetry project. The addition of a gas-uptake signal as a third independent measurement will allow deeper insight in complex reaction systems and may reveal effects that are not detectible if only the heat evaluation signal is measured.

Acknowledgment

We thank S. Petrozzi, H. P. Schläpfer, and M. Wohlwend for their great technical support, M. Linder and his staff (Mettler Toledo) for providing technical instrumentation and their suggestions for the succeeding of this work. We also thank three anonymous reviewers for their valuable comments on the paper.

Received for review May 18, 2004.

OP049900G